


High-order harmonic generation in three-dimensional Weyl semimetals with broken time-reversal symmetry

H. K. Avetissian, V. N. Avetisyan, B. R. Avchyan, and G. F. Mkrtchian ^{*}
Centre of Strong Fields Physics, Yerevan State University, Yerevan 0025, Armenia

 (Received 20 June 2022; accepted 1 September 2022; published 13 September 2022)

In this paper the nonlinear interaction of a Weyl semimetal (WSM) with a strong driving electromagnetic wave field is investigated. In the scope of the structure-gauge-invariant low-energy nonlinear electrodynamic theory, the polarization-resolved high-order harmonic generation spectra in the WSM with broken time-reversal symmetry are analyzed. The results obtained show that the spectra in the WSM are completely different compared to the two-dimensional graphene case. In particular, at the noncollinear arrangement of the electric and Weyl node momentum separation vectors, anomalous harmonics are generated which are polarized perpendicular to the pump wave electric field. The intensities of anomalous harmonics are quadratically dependent on the momentum space separation of the Weyl nodes. If the right and the left Weyl fermions are merged, we have a four-component trivial massless Dirac fermion and, as a consequence, the anomalous harmonics vanish. In contrast to the anomalous harmonics, the intensities of normal harmonics do not depend on the Weyl nodes' momentum separation vector and the harmonics spectra resemble the picture for a massless three-dimensional Dirac fermion.

DOI: [10.1103/PhysRevA.106.033107](https://doi.org/10.1103/PhysRevA.106.033107)

I. INTRODUCTION

As three-dimensional analogs of graphene [1,2], Dirac semimetals (DSMs) [3–6] and Weyl semimetals (WSMs) [7–12] have been implemented in a variety of condensed-matter systems. These materials are three-dimensional quantum phases of matter with gapless electronic excitations that are protected by topology and symmetry [13,14]. The low-energy dispersion of such materials contains conical intersections and diabolical points, which are referred to as Dirac points or a Weyl nodes [15]. The DSMs possess both time-reversal and spatial inversion symmetry. When one of these symmetries is broken, the Dirac points are split into a pair of Weyl nodes and the medium becomes a WSM. The low-energy theory of the simplest WSM is described by the Weyl Hamiltonian [16] near the Weyl nodes where the right-handed and left-handed chirality fermions are separated in the momentum space. Due to the nontrivial topology of the bands, the Berry curvature in the momentum space is nonzero [17,18] and we have an appropriate case of the Dirac monopole-antimonopole [19] realization in the momentum space [20]. As a result, the linear electromagnetic (EM) response of the three-dimensional WSM is described by an axionic field theory [21–23] with the anomalous linear electrodynamic effects [24–28]. The interaction between the strong EM waves and the WSM gives rise to nonlinear optical effects, such as the photovoltaic effect [29,30], optical rectification, second-harmonic generation [31–33], terahertz emission [34], and third harmonic generation [35]. These are perturbative nonlinear optical effects. With a further in-

crease of the driving wave intensity, the extreme nonlinear optical effects [36] may be visible in pseudorelativistic systems. In particular, high-order harmonic generation (HHG) is an essential nonlinear dynamic process that can be used as a probe to extract the properties of a medium. It can also be useful for new nanodevices. To date, HHG has been observed in graphene [37], DSMs [38,39], topological insulators [40], and WSMs [41], where the spikelike Berry curvature may generate even-order harmonics. Note that, as in graphene, there is quite a high carrier mobility in WSMs [42,43], that is, electrons can move significantly in the Brillouin zone, which is favorable for the HHG phenomenon in nanostructures.

As is well studied for graphene, the HHG process for the Dirac-cone approximation [44–49] is significantly different from HHG when electrons can move significantly in the Brillouin zone; here polarization and optical anisotropy effects of HHG in graphene arise [50–59]. The HHG in WSMs with a particular lattice realization was studied theoretically in Ref. [60], which reported anisotropic anomalous HHG from time-reversal symmetry-broken WSMs. The nonperturbative topological intraband current and transport in WSMs and DSMs in laser fields were investigated in Refs. [61,62]. The electron coherent dynamics in WSMs at the interaction with an ultrafast optical pulse was investigated in Ref. [63].

A nonlinear response intrinsically connected to topology should arise from the universal Weyl Hamiltonian, which is the root of the field theory anomalies. Hence, there is tremendous interest from a strong-field physics perspective in understanding how the field theory anomalies affect the nonlinear response of WSMs at low-energy excitations where the theory is universal and does not depend on the particular lattice realization of the WSM. To this end, in

^{*}mkrtchian@ysu.am

the present paper we investigate the low-energy nonlinear electrodynamics of WSMs with broken time-reversal symmetry and analyze polarization-resolved high-order harmonic generation spectra in WSMs. The consideration is based on the structure-gauge-invariant low-energy nonlinear electrodynamics where an ansatz applied to the Dirac monopole [64] is adopted to overcome the topological singularity.

The paper is organized as follows. In Sec. II the structure-gauge-invariant low-energy nonlinear electrodynamic theory with an evolutionary equation for the single-particle density matrix is presented. In Sec. III we consider polarization-resolved HHG spectra and present the main results. A summary is given in Sec. IV.

II. MODEL HAMILTONIAN AND EVOLUTIONARY EQUATION FOR THE SINGLE-PARTICLE DENSITY MATRIX

We start from the low-energy universal Hamiltonian involving the four-component massless Dirac fermion

$$\hat{H}_0 = v \int d^3x \bar{\Psi} (-i\gamma^j \partial_j + b_\mu \gamma^\mu \gamma^5) \Psi, \quad (1)$$

where v is the Fermi velocity, $\bar{\Psi} = \Psi^\dagger \gamma_0$, matrices γ^0 and γ^j ($j = 1, 2, 3$) are Dirac anticommuting γ matrices, $\gamma^5 = i\gamma^0 \gamma^1 \gamma^2 \gamma^3$ is the chirality matrix, and b_μ is the axial 4-vector. In the chiral representation of the γ matrices we have

$$\gamma^0 = \begin{pmatrix} 0 & 1 \\ 1 & 0 \end{pmatrix}, \quad \boldsymbol{\gamma} = \begin{pmatrix} 0 & \hat{\boldsymbol{\sigma}} \\ -\hat{\boldsymbol{\sigma}} & 0 \end{pmatrix}, \quad \gamma^5 = \begin{pmatrix} -1 & 0 \\ 0 & 1 \end{pmatrix}, \quad (2)$$

where $\hat{\boldsymbol{\sigma}}$ is the vector operator formed of three Pauli matrices. In Eq. (1) the term proportional to b_μ breaks charge, parity, or time-reversal symmetry. In this paper we consider the case of a spacelike axial vector $b_0 = 0$. In this case the axial vector term $\mathbf{b}\boldsymbol{\gamma}$ preserves inversion (\mathcal{P}) and charge conjugation (\mathcal{C}) symmetries, but breaks time-reversal symmetry (\mathcal{T}). Note that this case is more feasible for the realization of a Weyl semimetal and the corresponding minimal lattice model can easily be constructed [28]. The Hamiltonian (1) in the momentum space becomes

$$\hat{H}_0(\mathbf{k}) = v \begin{pmatrix} \boldsymbol{\sigma} \cdot (\mathbf{k} + \mathbf{b}) & 0 \\ 0 & -\boldsymbol{\sigma} \cdot (\mathbf{k} - \mathbf{b}) \end{pmatrix}. \quad (3)$$

For compactness of equations, atomic units are used throughout the paper unless otherwise indicated. The eigenstates of this Hamiltonian are also eigenstates of the chirality matrix γ^5 with eigenvalues $\chi = \pm 1$. Since the Dirac mass is zero, $\hat{H}_0(\mathbf{k})$ is block diagonal and the left-handed $(1 - \gamma^5)\Psi/2$ and right-handed $(1 + \gamma^5)\Psi/2$ components of the Dirac field are decoupled into left-handed and right-handed two-component Weyl spinors, described by the Hamiltonians [13,14,27,28]:

$$\hat{H}_\chi = -\chi v \boldsymbol{\sigma} \cdot (\mathbf{k} - \chi \mathbf{b}), \quad \chi = \pm 1. \quad (4)$$

The 2×2 Hamiltonians \hat{H}_1 and \hat{H}_{-1} also describe the monopole and the antimonopole of the Berry curvature in the momentum space, respectively [18,64]. For $\mathbf{b} \neq 0$, the right and the left Weyl fermions are separated in the momentum space and the WSM is topologically nontrivial. The momentum space separation of the Weyl nodes is $2|\mathbf{b}|$. The

eigenvalues $\chi = \pm 1$ also have a topological notion. The Berry flux piercing any surface enclosing the Weyl nodes $\mathbf{k} = \chi \mathbf{b}$ is exactly $2\pi\chi$, i.e., χ also defines the Chern number or topological charge. In accordance with the Nielsen-Ninomiya theorem, the Weyl nodes should come in opposite chirality pairs [65]. When $\mathbf{b} = 0$ these Weyl nodes are merged, giving rise to a topologically trivial, four-component massless Dirac fermion.

For the calculation of the nonlinear EM response of a WSM we need the eigenstates of the Hamiltonian (4). With these eigenstates we should calculate the Berry connection and then curvature. Because of the monopole in momentum space, the eigenstates of the Weyl Hamiltonian (4) cannot be defined globally for all \mathbf{k} . The eigenstates $|\beta, \chi, \mathbf{k}\rangle$, where β refers to the band index, can be subject to an arbitrary structure-gauge [66] transformation

$$|\beta, \chi, \mathbf{k}'\rangle = \mathbf{e}^{i\vartheta_{\chi\beta}(\mathbf{k})} |\beta, \chi, \mathbf{k}\rangle \quad (5)$$

without changing the physical properties of the system. For the quantum kinetics we need to calculate the transition dipole moments $\mathbf{d}_{\beta\beta'}(\chi, \mathbf{k}) = \langle \beta, \chi, \mathbf{k} | i\partial_{\mathbf{k}} | \beta', \chi, \mathbf{k} \rangle$. The Berry connections are defined as the diagonal elements $\mathbf{A}_\beta(\chi, \mathbf{k}) = \mathbf{d}_{\beta\beta}(\chi, \mathbf{k})$. Hence, due to the gradient $\partial_{\mathbf{k}}$, a smooth structure gauge for the eigenstates is thus required. To overcome this problem we will adopt the ansatz applied to the Dirac monopole. To this end we choose the axial vector \mathbf{b} directed along the x axis $\mathbf{b} = b\hat{\mathbf{x}}$ and define the eigenstates for $k_z \geq 0$ and $k_z \leq 0$. Since $\hat{H}_{\chi=-1}(-\mathbf{k}) = \hat{H}_{\chi=1}(\mathbf{k})$ we will arrive at the solution for the left-handed Weyl spinors. The eigenstates $|\beta, \chi, \mathbf{k}\rangle_+$ for $k_z \geq 0$ are

$$|c, \chi, \mathbf{k}\rangle_+ = \frac{1}{\sqrt{2k_\chi^2 + 2k_\chi k_z}} \begin{bmatrix} k_\chi + k_z \\ k_{x\chi} + ik_y \end{bmatrix}, \quad (6)$$

$$|v, \chi, \mathbf{k}\rangle_+ = \frac{1}{\sqrt{2k_\chi^2 + 2k_\chi k_z}} \begin{bmatrix} -k_{x\chi} + ik_y \\ k_\chi + k_z \end{bmatrix}; \quad (7)$$

for $k_z \leq 0$ we have

$$|c, \chi, \mathbf{k}\rangle_- = \frac{1}{\sqrt{2k_\chi^2 - 2k_\chi k_z}} \begin{bmatrix} k_{x\chi} - ik_y \\ k_\chi - k_z \end{bmatrix}, \quad (8)$$

$$|v, \chi, \mathbf{k}\rangle_- = \frac{1}{\sqrt{2k_\chi^2 - 2k_\chi k_z}} \begin{bmatrix} -k_\chi + k_z \\ k_{x\chi} + ik_y \end{bmatrix}, \quad (9)$$

where $k_{x\chi} = k_x - \chi b$ and $k_\chi = \sqrt{k_{x\chi}^2 + k_y^2 + k_z^2}$. The eigenenergies are $\mathcal{E}_{c\chi}(\mathbf{k}) = vk_\chi$ and $\mathcal{E}_{v\chi}(\mathbf{k}) = -vk_\chi$.

The solutions for the opposite chirality are $|c, \chi, \mathbf{k}\rangle_\pm = |c, -\chi, -\mathbf{k}\rangle_\mp$ and $|v, \chi, \mathbf{k}\rangle_\pm = |v, -\chi, -\mathbf{k}\rangle_\mp$. At the overlap $k_z = 0$ solutions Eqs. (6) and (8) and Eqs. (7) and (9) are connected by the gauge transformation

$$|c, \chi, \mathbf{k}\rangle_- = e^{-i\vartheta(k_{x\chi}, k_y)} |c, \chi, \mathbf{k}\rangle_+,$$

$$|v, \chi, \mathbf{k}\rangle_- = e^{i\vartheta(k_{x\chi}, k_y)} |v, \chi, \mathbf{k}\rangle_+,$$

where $\vartheta(k_{x\chi}, k_y) = \arctan(k_y/k_{x\chi})$. From Eqs. (6) and (8) and Eqs. (7) and (9) for the total Berry connection $\mathbf{A}(\chi, \mathbf{k}) = \langle c, \chi, \mathbf{k} | i\partial_{\mathbf{k}} | c, \chi, \mathbf{k} \rangle - \langle v, \chi, \mathbf{k} | i\partial_{\mathbf{k}} | v, \chi, \mathbf{k} \rangle$ we obtain

$$A_+(\chi, \mathbf{k}) = -\chi \frac{k_y \hat{\mathbf{x}} - k_{x\chi} \hat{\mathbf{y}}}{k_\chi^2 + k_\chi k_z}, \quad (10)$$

$$A_-(\chi; \mathbf{k}) = \chi \frac{k_y \hat{\mathbf{x}} - k_x \chi \hat{\mathbf{y}}}{k_x^2 - k_x k_z}. \quad (11)$$

For the Berry curvature $\mathcal{B}(\chi; \mathbf{k}) = \partial \mathbf{k} \times \mathcal{A}(\chi, \mathbf{k})$ we obtain, located at the Weyl node $\mathbf{k} = \chi \mathbf{b}$, the monopole field

$$B_x = \chi \frac{k_x \chi}{k_x^3}, \quad B_y = \chi \frac{k_y}{k_x^3}, \quad B_z = \chi \frac{k_z}{k_x^3}, \quad (12)$$

where $\text{div} \mathcal{B} = 4\pi \chi \delta(\mathbf{k} - \chi \mathbf{b})$ and δ is the Dirac delta function. For the transition dipole moments we have

$$\begin{aligned} \mathbf{d}_{cv_+}(\chi, \mathbf{k}) &= \frac{(ik_{x\chi} - \chi k_y) \hat{\mathbf{z}}}{2k_x^2} + \frac{1}{2k_x(k_x + k_z)} \\ &\times \left\{ \left[i \left(\frac{k_{x\chi}^2}{k_x} - k_x - k_z \right) - \frac{\chi k_y k_{x\chi}}{k_x} \right] \hat{\mathbf{x}} \right. \\ &\left. + \left[\chi \left(k_x + k_z - \frac{k_y^2}{k_x} \right) + i \frac{k_{x\chi} k_y}{k_x} \right] \hat{\mathbf{y}} \right\}, \quad (13) \\ \mathbf{d}_{cv_-}(\chi, \mathbf{k}) &= \frac{(ik_{x\chi} + \chi k_y) \hat{\mathbf{z}}}{2k_x^2} - \frac{1}{2k_x(k_x - k_z)} \\ &\times \left\{ \left[\chi \frac{k_y k_{x\chi}}{k_x} + i \left(\frac{k_{x\chi}^2}{k_x} - k_x + k_z \right) \right] \hat{\mathbf{x}} \right. \\ &\left. - \left[\chi \left(k_x - k_z - \frac{k_y^2}{k_x} \right) - \frac{ik_{x\chi} k_y}{k_x} \right] \hat{\mathbf{y}} \right\}. \quad (14) \end{aligned}$$

Note the useful relation

$$\begin{aligned} \frac{1}{2} \epsilon^{abc} B^c(\chi, \mathbf{k}) \\ = i \{ d_{cv}^a(\chi, \mathbf{k}) d_{vc}^b(\chi, \mathbf{k}) - d_{cv}^b(\chi, \mathbf{k}) d_{vc}^a(\chi, \mathbf{k}) \}, \quad (15) \end{aligned}$$

where ϵ^{abc} is the Levi-Civita symbol and the summation over the repeated upper indices is implied. This equation is gauge invariant and connects the transition dipole moments with the Berry curvature. Here, for the sake of brevity, we omit the indices \pm .

The semiconductor Bloch equations (SBEs) governing a WSM driven by a strong laser field in the length gauge read

$$\begin{aligned} \partial_t \rho_{\alpha\beta;\chi}(\mathbf{k}_0, t) &= i E_{\beta\alpha;\chi}(\mathbf{k}_0 + \mathbf{A}) \rho_{\alpha\beta;\chi}(\mathbf{k}_0, t) \\ &- (1 - \delta_{\alpha\beta}) \Gamma \rho_{\alpha\beta;\chi}(\mathbf{k}_0, t) \\ &+ i \left[\sum_{\alpha'} \mathbf{d}_{\alpha'\beta}(\chi, \mathbf{k}_0 + \mathbf{A}) \rho_{\alpha\alpha';\chi}(\mathbf{k}_0, t) \right. \\ &\left. - \sum_{\beta'} \mathbf{d}_{\alpha\beta'}(\chi, \mathbf{k}_0 + \mathbf{A}) \rho_{\beta'\beta;\chi}(\mathbf{k}_0, t) \right] \mathbf{E}(t), \quad (16) \end{aligned}$$

where $\rho_{\alpha\beta;\chi}$ are the single-particle density-matrix elements, \mathbf{E} is the laser electric-field strength, $\mathbf{A} = -\int_0^t \mathbf{E}(t') dt'$ is the vector potential, $\mathcal{E}_{\beta\alpha;\chi}(\mathbf{k}) = \mathcal{E}_{\beta\chi}(\mathbf{k}) - \mathcal{E}_{\alpha\chi}(\mathbf{k})$, and Γ^{-1} is the dephasing time. The crystal momentum \mathbf{k} has been transformed into a frame moving with the vector potential $\mathbf{k}_0 = \mathbf{k} - \mathbf{A}$. Note that in Eq. (16), the Berry connections (10) and (11) are included, $\mathbf{d}_{\beta\beta}(\chi, \mathbf{k}) \hat{=} \mathbf{A}_{\beta}(\chi, \mathbf{k})$.

The optical excitation induces a volume current that can be calculated by the formula

$$\begin{aligned} \mathbf{j}(t) &= - \left[\sum_{\alpha\chi\mathbf{k}_0} [\mathbf{V}_{\alpha\chi}(\mathbf{k}_0 + \mathbf{A})] \rho_{\alpha\alpha;\chi}(\mathbf{k}_0, t) \right. \\ &+ i \sum_{\alpha \neq \beta, \chi} \sum_{\mathbf{k}_0} \mathbf{d}_{\beta\alpha}(\chi, \mathbf{k}_0 + \mathbf{A}) \\ &\left. \times E_{\beta\alpha;\chi}(\mathbf{k}_0 + \mathbf{A}) \rho_{\alpha\beta;\chi}(\mathbf{k}_0, t) \right], \quad (17) \end{aligned}$$

where the band velocity is defined by $\mathbf{V}_{\alpha\chi}(\mathbf{k}) = \partial_{\mathbf{k}} \mathcal{E}_{\alpha\chi}(\mathbf{k})$. Note that Eqs. (16) and (17) provide structure-gauge-invariant kinetic theory. Thus, at the structure-gauge transformation (5) we have

$$\mathbf{d}'_{\alpha\beta}(\chi, \mathbf{k}) = e^{i\theta_{\chi\beta}(\mathbf{k}) - i\theta_{\chi\alpha}(\mathbf{k})} \mathbf{d}_{\alpha\beta}(\chi, \mathbf{k}),$$

$$\mathcal{A}'_{\alpha}(\chi, \mathbf{k}) = \mathcal{A}_{\alpha}(\chi, \mathbf{k}) - \partial_{\mathbf{k}} \theta_{\chi\alpha}(\mathbf{k}), \quad \mathcal{B}'(\chi; \mathbf{k}) = \mathcal{B}(\chi; \mathbf{k}),$$

$$\rho'_{\alpha\beta;\chi}(\mathbf{k}_0, t) = e^{i\theta_{\beta}(\mathbf{k}_0 + \mathbf{A}) - i\theta_{\alpha}(\mathbf{k}_0 + \mathbf{A})} \rho_{\alpha\beta;\chi}(\mathbf{k}_0, t),$$

$$\mathbf{j}'(t) = \mathbf{j}(t).$$

III. RESULTS

We explore the nonlinear response of a WSM in a laser field of ultrashort duration

$$\mathbf{E}(t) = f(t) E_0 \hat{\mathbf{e}} \cos(\omega t), \quad (18)$$

where $f(t) = \sin^2(\pi t/\tau)$ is the sin-squared envelope function, τ is the pulse duration, $\hat{\mathbf{e}}$ is the unit polarization vector, ω is the carrier frequency, and E_0 is the electric-field amplitude. We use a ten-cycle fundamental laser field.

As in graphene, the wave-particle interaction in a WSM is characterized by the dimensionless parameter [45]

$$\xi_0 = \frac{e E_0 v T}{\hbar \omega}, \quad (19)$$

which represents the work of the wave electric field E_0 on a period $T = 2\pi/\omega$ in the units of photon energy $\hbar\omega$. The parameter is written here in general units for clarity. For a two-band WSM system the SBEs (16) are reduced to a closed set of equations for the interband polarization $P_{\chi}(\mathbf{k}_0, t) \equiv \rho_{vc;\chi}(\mathbf{k}_0, t)$ and for the distribution functions $N_{c(v)}(\mathbf{k}_0, t) \equiv \rho_{cc(vv);\chi}(\mathbf{k}_0, t)$ in the conduction (valence) bands. For an undoped system in equilibrium, the initial conditions $P_{\chi}(\mathbf{k}_0, 0) = 0$, $N_c(\mathbf{k}_0, 0) = 0$, and $N_v(\mathbf{k}_0, 0) = 1$ are assumed, neglecting thermal occupations. The integration of the SBEs is performed on a three-dimensional grid of $500 \times 500 \times 500$ points homogeneously distributed in the cube $(-\alpha_{\text{cut}}\omega/v, \alpha_{\text{cut}}\omega/v)_{XYZ}$. The minimum or maximum crystal momentum is defined by α_{cut} , which in turn depends on the intensity of the pump wave. The time integration is performed with the standard fourth-order Runge-Kutta algorithm. From Eq. (17) follows the relation

$$\frac{d\mathbf{j}(t)}{dt} \frac{(2\pi)^3 v^2}{\omega^4} = \mathbf{w} \left(\bar{t}, \xi_0, \frac{bv}{\omega}, \frac{\Gamma}{\omega} \right), \quad (20)$$

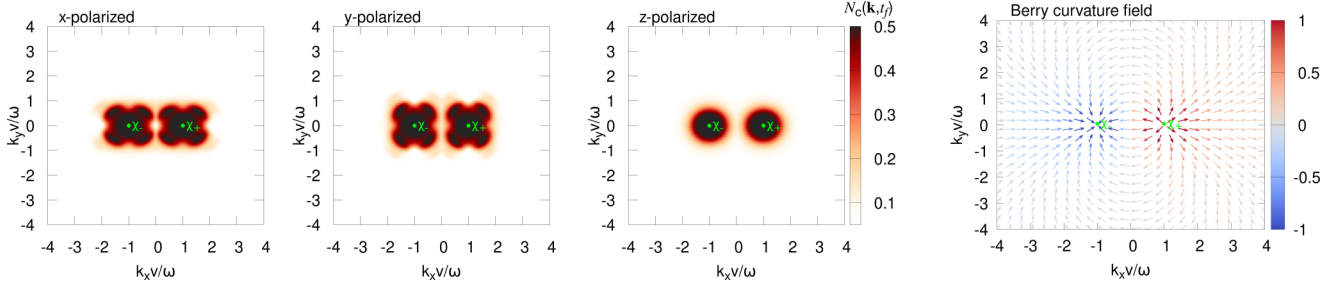


FIG. 1. Particle distribution function $N_c(\mathbf{k}, t_f)$ (in arbitrary units) in the plane $k_z = 0$ after the interaction at the instant $t_f = \tau$ for a WSM, as a function of scaled dimensionless momentum components ($k_x v/\omega$ and $k_y v/\omega$) for different orientations of the laser electric-field strength. The wave-particle dimensionless interaction parameter is taken to be $\xi_0 = 0.5$ and the axial vector magnitude is chosen to be $b = \omega/v$. The Weyl nodes are located at $k_x v/\omega = \pm 1$. The rightmost panel shows the Berry curvature normalized vector field (in arbitrary units) in the plane $k_z = 0$. The Weyl points are the sink and source of the Berry curvature.

where $\bar{t} = \omega t$ and $\mathbf{w}(\bar{t}, \xi_0, \frac{bv}{\omega}, \frac{\Gamma}{\omega})$ is a periodic (in the case of an external monochromatic wave) dimensionless universal function that parametrically depends on the WSM-wave interaction parameters ξ_0 , the scaled axial vector, and the scaled relaxation rate. Hence, by solving the SBEs (16), performing the integral over \mathbf{k}_0 (17), and taking Fourier transform \mathcal{F} , the polarization-resolved high-harmonic spectrum is calculated as

$$I_\alpha = \left| \mathcal{F} \left(w_\alpha \left(\bar{t}, \xi_0, \frac{bv}{\omega}, \frac{\Gamma}{\omega} \right) \right) \right|^2, \quad \alpha = x, y, z. \quad (21)$$

For all calculations, the relaxation time is taken to be equal to half of the wave period $\Gamma^{-1} = T/2 = \pi/\omega$.

The typical photoexcitation of the Fermi-Dirac sea is presented in Fig. 1, which shows the density plot of the particle distribution function $N_c(\mathbf{k}, t_f)$ after the interaction at the instant $t_f = 10T$, as a function of dimensionless momentum components, for different orientations of the laser electric-field strength. As can be seen from this figure, near the Weyl nodes we have an almost homogeneous excitation due to the singularity of the transition dipole moments. Far from the Weyl nodes the excitation pattern is defined by the anisotropy of the transition dipole moments (13) and (14). The rightmost panel of Fig. 1 shows the Berry curvature vector field. The Weyl points are the sink and source of the Berry curvature. The Berry curvature can be thought of as an effective magnetic field, which will initiate Hall current perpendicular to the applied electric field. Figure 2 shows the polarization-resolved HHG spectra in logarithmic scale for a WSM in the strong-field regime for different orientations of the laser electric-field strength. From top to bottom we show the spectra for the x , y , and z polarizations of the pump wave. As can be seen from this figure, when the driving wave is polarized in the x direction, the odd harmonics are generated only in the laser polarization direction. However, when the wave is polarized in the y or z direction, in addition to normal harmonics generated along the laser polarization, anomalous harmonics in perpendicular directions are also generated. As reflected from Fig. 2, anomalous harmonics are generated at the noncollinear arrangement of the electric field and the Weyl node's momentum separation vectors. This is a manifestation of the axionic field theory with anomalous nonlinear electrodynamic effects.

To understand how these findings are related to the non-trivial topology of a WSM, let us derive another equivalent

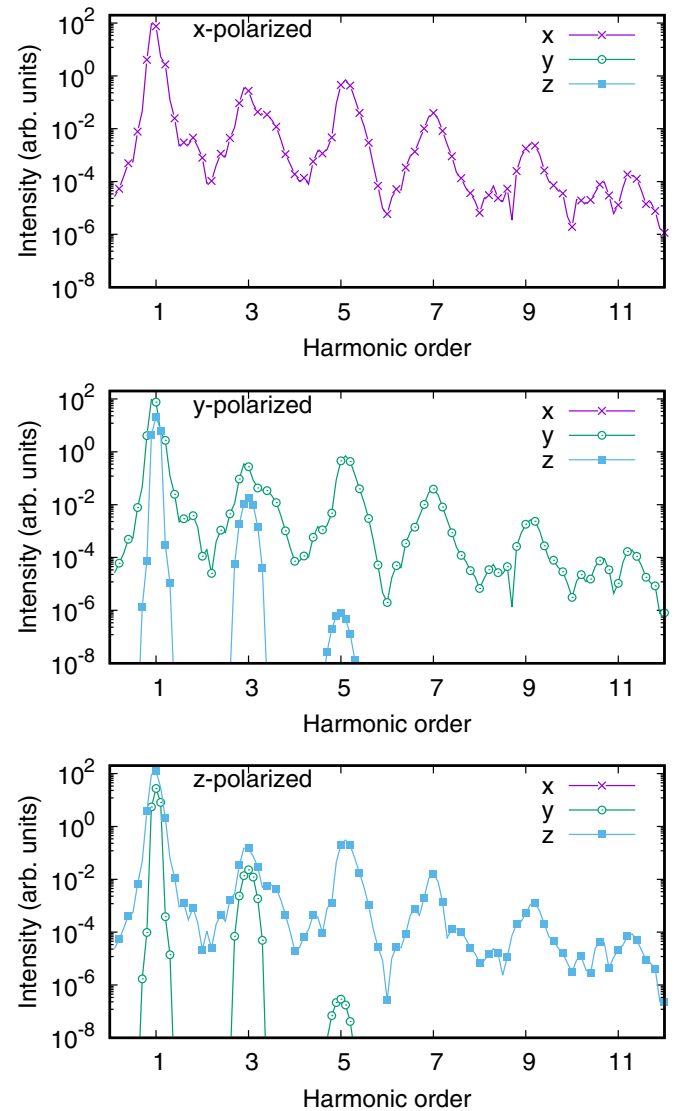


FIG. 2. Polarization resolved HHG spectra in logarithmic scale for a WSM in the strong-field regime for different orientations of the laser electric-field strength. The wave-particle dimensionless interaction parameter is taken to be $\xi_0 = 0.5$ and the axial vector magnitude is chosen to be $b = \omega/2v$. The Weyl nodes are located at $k_x v/\omega = \pm 0.5$.

equation for the current (17) that explicitly includes Berry curvature (12). From Eq. (16), inserting the expression for $i\mathcal{E}_{\beta\alpha\chi}(\mathbf{k}_0 + \mathbf{A})\rho_{\alpha\beta;\chi}(\mathbf{k}_0, t)$ into the equation for the current (17) and taking into account the relation (15), electron-hole symmetry $\mathbf{V}_{v\chi} = -\mathbf{V}_{c\chi}$, and the integral of motion $N_{v;\chi}(\mathbf{k}_0, t) + N_{c;\chi}(\mathbf{k}_0, t) = 1$, we find

$$\begin{aligned}
j_a(t) = & -2 \sum_{\chi \mathbf{k}_0} V_{c\chi}^a N_{c;\chi}(\mathbf{k}_0, t) \\
& - 2 \operatorname{Re} \sum_{\chi \mathbf{k}_0} d_{cv}^a(\chi, \mathbf{k}_0 + \mathbf{A}) \{ \partial_t P_\chi(\mathbf{k}_0, t) + \Gamma P_\chi(\mathbf{k}_0, t) \} \\
& + 2 \operatorname{Re} \sum_{\chi \mathbf{k}_0} i E^b(t) \mathcal{A}^b(\chi, \mathbf{k}_0 + \mathbf{A}) d_{cv}^a(\chi, \mathbf{k}_0 + \mathbf{A}) \\
& \times P_\chi(\mathbf{k}_0, t) \\
& + \sum_{\chi \mathbf{k}_0} \frac{1}{2} \epsilon^{abc} E^b(t) \mathcal{B}^c(\chi, \mathbf{k}_0 + \mathbf{A}) \\
& - \sum_{\chi \mathbf{k}_0} \epsilon^{abc} E^b(t) \mathcal{B}^c(\chi, \mathbf{k}_0 + \mathbf{A}) N_{c;\chi}(\mathbf{k}_0, t), \quad (22)
\end{aligned}$$

where the summation over the repeated upper indices is implied. The first term in Eq. (22) is the ordinary intraband part of the current, the second and third terms define the interband part of the current, and the fourth and fifth terms represent the topological part of the current. These terms are defined by the Berry curvature (12). The fourth term is nothing but the anomalous Hall current [27,28] and depends linearly on the field strength E , since $\sum_{\chi \mathbf{k}_0} \mathcal{B}^c(\chi, \mathbf{k}_0 + \mathbf{A}) = \sum_{\chi \mathbf{k}} \mathcal{B}^c(\chi, \mathbf{k})$. The last term in Eq. (22) is the nonlinear part of the anomalous Hall current that gives rise to anomalous harmonics perpendicular to the laser field strength directions: $\epsilon^{abc} E^b \mathcal{B}^c = \mathbf{E} \times \mathcal{B}$. From the vector field structure (cf. Fig. 1) of Berry curvature, it is clearly seen that the x component does not change the sign away from the Weyl nodes along the k_x axis, while the y component changes the sign along the k_y axis. Thus, if the driving wave is polarized along the axial vector \mathbf{b} (x direction), then it is easy to see that the anomalous current in the y and z directions turns out to be zero as the monopole fields (12) of Weyl nodes cancel each other. On the other hand, when the driving wave is polarized in the y or z direction, then the x component of the Berry curvature comes into play. Let us analyze for concreteness the case of the z -polarized driving wave. In this case the anomalous Hall current can be written

$$\begin{aligned}
j_y = & \frac{E^z(t)}{(2\pi)^3} \int d^3 \mathbf{k}_0 \\
& \times \left[\frac{(k_{0x} + b) N_{c;1}(\mathbf{k}_0, t)}{\sqrt{(k_{0x} + b)^2 + k_{0y}^2 + (k_{0z} + A_z)^2}} - (b \rightarrow -b) \right]. \quad (23)
\end{aligned}$$

At the first glance, for each Weyl node taking into account unbounded linear dispersion of fermions, one can make a naive shift of the variable $k_{x\chi} = k_x - \chi b$ and make this integral vanish. However, we should take into account singularity near $\pm b$ points as in the case of linear axionic field theory [27]. Therefore, we need to choose a finite cutoff along the axial vector (x direction), which can be sent to infinity at the end of

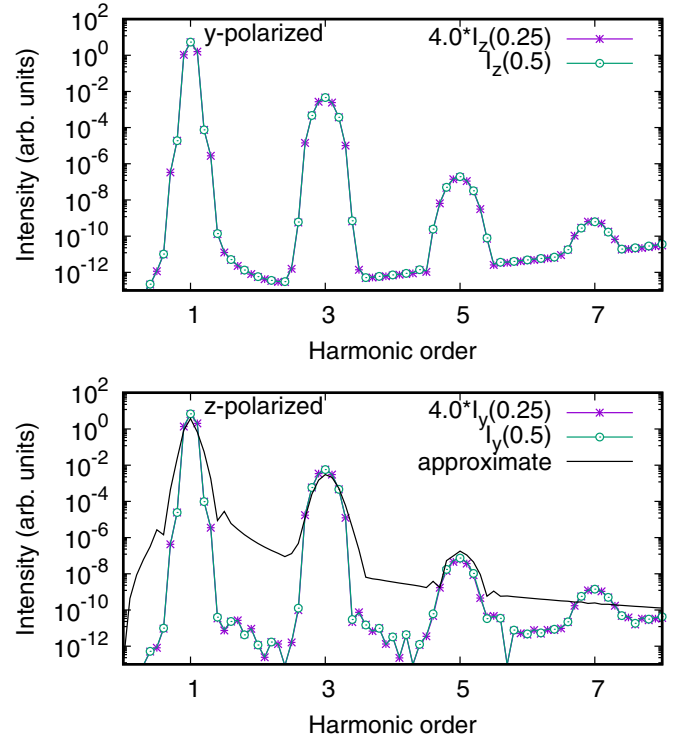


FIG. 3. Anomalous HHG spectra in logarithmic scale for a WSM in the strong-field regime for different axial vector magnitudes $bv/\omega = 0.25$ and 0.5 . The wave-particle dimensionless interaction parameter is taken to be $\xi_0 = 1.0$. The black solid line for the z polarization of the pump wave corresponds to the approximate result (24).

calculations and can keep the cutoffs infinite in the directions perpendicular to the axial vector. As reflected from Fig. 1, near the Weyl nodes we have an almost homogeneous excitation due to the singularity of the transition dipole moments (13) and (14). Hence, we can approximate the integral (23) as

$$\begin{aligned}
j_y \simeq & \frac{2}{(2\pi)^3} E^z(t) N_{c;1}(\mathbf{k}_{0w}, t) \\
& \times \int_0^\infty k_\perp dk_\perp \int_{-\Lambda}^\Lambda dk_{0x} \int_0^{2\pi} d\phi \frac{k_{0x} + b}{[k_\perp^2 + (k_{0x} + b)^2]^{3/2}} \\
= & \frac{2}{(2\pi)^2} E^z(t) N_{c;1}(\mathbf{k}_{0w}, t) \int_{-\Lambda}^\Lambda \operatorname{sgn}(k_{0x} + b) dk_{0x} \\
= & \frac{b}{\pi^2} E^z(t) N_{c;1}(\mathbf{k}_{0w}, t), \quad (24)
\end{aligned}$$

where $N_{c;1}(\mathbf{k}_{0w}, t) = N_{c;1}(\mathbf{k}_w - \mathbf{A}, t)$ is calculated near the Weyl node $\mathbf{k}_w = (b, 0, 0)$. This is an interesting result which implies that the nonlinear anomalous Hall current is proportional to the axial vector as in the linear axionic field theory. However, this result is only valid for the unbounded linear dispersion of the Weyl fermions. If we consider a lattice model of a WSM, the linear dispersion is valid only near the Weyl nodes and integration is performed over the finite Brillouin zone. Therefore, the nonlinear anomalous Hall current of a WSM at high energies will be modified by a nonlinear contribution from the axial vector. Figure 3 presents the anomalous

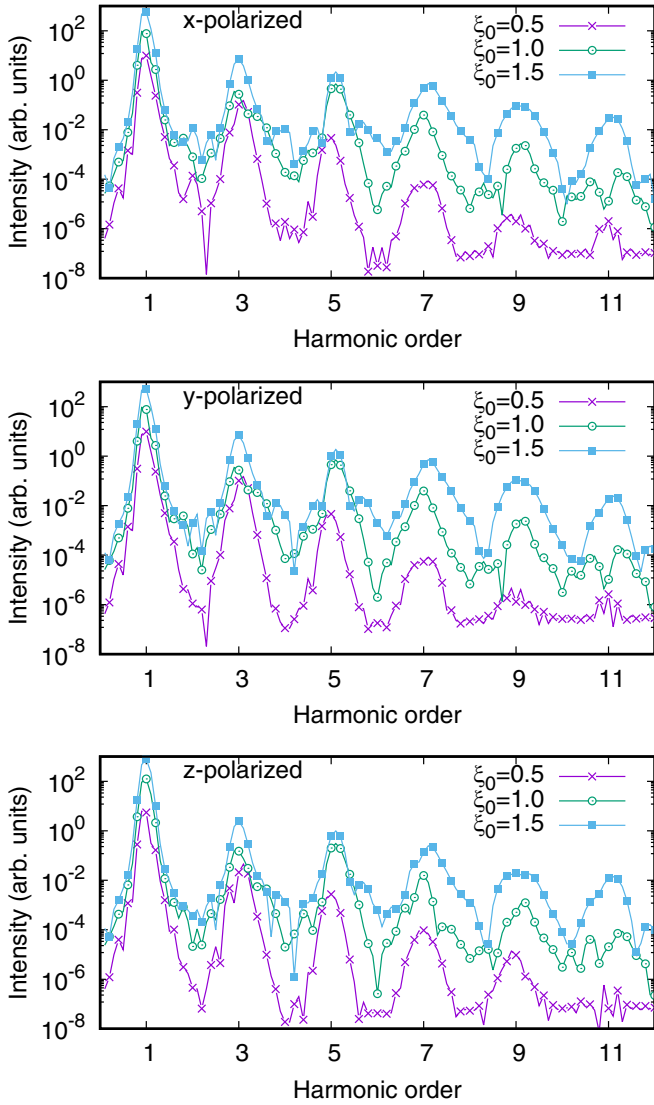


FIG. 4. The HHG spectra for the normal harmonics in logarithmic scale for a WSM in the strong-field regime for different orientations of the pump laser electric-field strength at various values of the wave-particle dimensionless interaction parameter ξ_0 .

HHG spectra in logarithmic scale for a WSM in the strong-field regime, for different axial vector magnitudes, calculated with the help of Eq. (17). The results for $bv/\omega = 0.25$ are multiplied by the factor 4. As can be seen from Fig. 3, the intensities of anomalous harmonics are quadratically dependent on the momentum space separation of the Weyl nodes. Also presented in Fig. 3 is the result calculated with the help of the approximate formula (24). As can be seen from this figure, the approximate curve reproduces well the exact numerical results for low harmonics but fails at higher harmonics, since higher harmonics being more sensitive to the time variation of the particle distribution function $N_c(\mathbf{k}, t_f)$ require a more accurate approach. The obtained anomalous harmonics' dependence on the distance between the Weyl nodes in reciprocal space differs from the case of the lattice model [60] where the intensity of anomalous harmonics decreases with the increasing distance between the Weyl nodes. It is

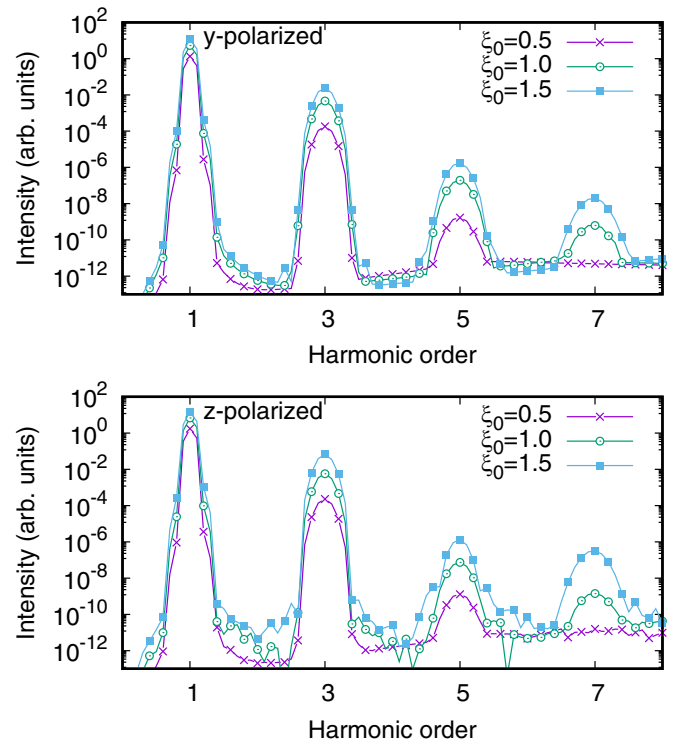


FIG. 5. The HHG spectra for the anomalous harmonics in logarithmic scale for a WSM in the strong-field regime for different orientations of the pump laser electric-field strength at various values of the wave-particle dimensionless interaction parameter ξ_0 . The Weyl nodes are located at $k_x v/\omega = \pm 0.5$.

straightforward to see that for the normal harmonics with the shift of variable $k_{x\chi} = k_x - \chi b$ one can obtain results independent of b . This is equivalent to the fact that the right and the left Weyl fermions are merged and we have a four-component trivial massless Dirac fermion; as a consequence, the anomalous harmonics vanish. In addition, the intensities of normal harmonics do not depend on the Weyl node's momentum separation vector and resemble the results for a massless three-dimensional Dirac fermion.

We now turn to an examination of the effect of the driving wave intensity on the HHG in a WSM. We present the results of simulations for normal harmonics at different polarizations in Fig. 4. The intensities of normal harmonics I_α do not depend on the Weyl node's location. For the considered intensities the perturbation theory is not applicable, and in Fig. 4 we have a strong deviation from the power law for the intensities of harmonics. In particular, the intensities of the fifth, seventh, and ninth harmonics scale as $I_5 \sim \xi_0^3$, $I_7 \sim \xi_0^7$, and $I_9 \sim \xi_0^9$, respectively, whereas they should show the $I_n \sim \xi_0^{2n}$ dependence in the perturbative limit. In addition, this figure shows that the intensities of the normal harmonics are almost independent of the pump wave polarization, which is connected with the isotropic linear dispersion of the Weyl fermions.

Figure 5 shows the HHG spectra for the anomalous harmonics for a WSM in the strong-field regime for different orientations of the pump laser electric-field strength at various values of the wave-particle dimensionless interaction parameter ξ_0 . The Weyl nodes are located at $k_x v/\omega = \pm 0.5$. In this

case, we also have a strong deviation from the power law for the intensities of anomalous harmonics. In particular, the intensities of the third, fifth, and seventh harmonics scale as $I_3 \sim \xi_0^4$, $I_5 \sim \xi_0^6$, and $I_7 \sim \xi_0^8$, respectively. The dependences of the intensities of normal and anomalous harmonics on the intensity of the driving wave are completely different, which is due to the different underlying mechanisms.

IV. CONCLUSION

We have presented a structure-gauge-invariant microscopic theory of nonlinear interaction of a time-reversal symmetry-broken WSM with a strong low-frequency driving pulse of linear polarization. We numerically solved the semiconductor Bloch equations governing a WSM driven by a strong laser field in the length gauge and considered the HHG process depending on the Weyl node's momentum separation vector and the driving wave intensity. Our results show that at the noncollinear arrangement of the electric field and Weyl node's momentum separation vectors, anomalous harmonics are

generated which are polarized perpendicular to the direction of the pump wave electric field. The intensities of anomalous harmonics are quadratically dependent on the momentum space separation of the Weyl nodes. When the right and the left Weyl fermions are merged, the anomalous harmonics vanish. In contrast to the anomalous harmonics, the intensities of normal harmonics do not depend on the Weyl node's momentum separation vector. The dependences of the intensities of the normal and anomalous harmonics on the intensity of the driving wave are completely different, and for moderately strong driving waves one can enter an extreme nonlinear regime of HHG. The results of the present investigation not only are of theoretical and academic importance, but also will have significant implications for the rapidly developing area of modern extreme nonlinear optics of topological nanomaterials.

ACKNOWLEDGMENTS

The work was supported by the Science Committee of Republic of Armenia, Project No. 21AG-1C014.

-
- [1] K. S. Novoselov, A. K. Geim, S. V. Morozov, D. Jiang, M. I. Katsnelson, I. V. Grigorieva, S. V. Dubonos, and A. A. Firsov, *Nature (London)* **438**, 197 (2005).
- [2] A. H. Castro Neto, F. Guinea, N. M. R. Peres, K. S. Novoselov, and A. K. Geim, *Rev. Mod. Phys.* **81**, 109 (2009).
- [3] S. Borisenko, Q. Gibson, D. Evtushinsky, V. Zabolotnyy, B. Buchner, and R. J. Cava, *Phys. Rev. Lett.* **113**, 027603 (2014).
- [4] Z. Liu, J. Jiang, B. Zhou, Z. Wang, Y. Zhang, H. Weng, D. Prabhakaran, S. Mo, H. Peng, P. Dudin *et al.*, *Nat. Mater.* **13**, 677 (2014).
- [5] Z. Liu, B. Zhou, Y. Zhang, Z. Wang, H. Weng, D. Prabhakaran, S.-K. Mo, Z. Shen, Z. Fang, X. Dai *et al.*, *Science* **343**, 864 (2014).
- [6] M. Neupane, S.-Y. Xu, R. Sankar, N. Alidoust, G. Bian, C. Liu, I. Belopolski, T.-R. Chang, H.-T. Jeng, H. Lin *et al.*, *Nat. Commun.* **5**, 3786 (2014).
- [7] S.-M. Huang, S.-Y. Xu, I. Belopolski, C.-C. Lee, G. Chang, B. Wang, N. Alidoust, G. Bian, M. Neupane, C. Zhang *et al.*, *Nat. Commun.* **6**, 7373 (2015).
- [8] B. Q. Lv, H. M. Weng, B. B. Fu, X. P. Wang, H. Miao, J. Ma, P. Richard, X. C. Huang, L. X. Zhao, G. F. Chen, Z. Fang, X. Dai, T. Qian, and H. Ding, *Phys. Rev. X* **5**, 031013 (2015).
- [9] B. Lv, N. Xu, H. Weng, J. Ma, P. Richard, X. Huang, L. Zhao, G. Chen, C. Matt, F. Bisti *et al.*, *Nat. Phys.* **11**, 724 (2015).
- [10] S.-Y. Xu, N. Alidoust, I. Belopolski, Z. Yuan, G. Bian, T.-R. Chang, H. Zheng, V. N. Strocov, D. S. Sanchez, G. Chang *et al.*, *Nat. Phys.* **11**, 748 (2015).
- [11] S.-Y. Xu, I. Belopolski, N. Alidoust, M. Neupane, G. Bian, C. Zhang, R. Sankar, G. Chang, Z. Yuan, C.-C. Lee *et al.*, *Science* **349**, 613 (2015).
- [12] N. Xu, H. Weng, B. Lv, C. Matt, J. Park, F. Bisti, V. Strocov, D. Gawryluk, E. Pomjakushina, K. Conder *et al.*, *Nat. Commun.* **7**, 11006 (2016).
- [13] N. P. Armitage, E. J. Mele, and A. Vishwanath, *Rev. Mod. Phys.* **90**, 015001 (2018).
- [14] M. Z. Hasan, S.-Y. Xu, I. Belopolski, and S.-M. Huang, *Annu. Rev. Condens. Matter Phys.* **8**, 289 (2017).
- [15] X. Wan, A. M. Turner, A. Vishwanath, and S. Y. Savrasov, *Phys. Rev. B* **83**, 205101 (2011).
- [16] H. Weyl, *Proc. Natl. Acad. Sci. USA* **15**, 323 (1929).
- [17] M. V. Berry, *Proc. R. Soc. London Ser. A* **392**, 45 (1984).
- [18] D. Xiao, M.-C. Chang, and Q. Niu, *Rev. Mod. Phys.* **82**, 1959 (2010).
- [19] P. A. M. Dirac, *Proc. R. Soc. London Ser. A* **133**, 60 (1931).
- [20] Z. Fang, N. Nagaosa, K. S. Takahashi, A. Asamitsu, R. Mathieu, T. Ogasawara, H. Yamada, M. Kawasaki, Y. Tokura, and K. Terakura, *Science* **302**, 92 (2003).
- [21] S. Adler, *Phys. Rev.* **177**, 2426 (1969).
- [22] J. S. Bell and R. Jackiw, *Nuovo Cimento A* **60**, 47 (1969).
- [23] F. Wilczek, *Phys. Rev. Lett.* **58**, 1799 (1987).
- [24] A. A. Zyuzin and A. A. Burkov, *Phys. Rev. B* **86**, 115133 (2012).
- [25] D. T. Son and N. Yamamoto, *Phys. Rev. Lett.* **109**, 181602 (2012).
- [26] Z. Wang and S. C. Zhang, *Phys. Rev. B* **87**, 161107(R) (2013).
- [27] P. Goswami and S. Tewari, *Phys. Rev. B* **88**, 245107 (2013).
- [28] M. M. Vazifeh and M. Franz, *Phys. Rev. Lett.* **111**, 027201 (2013).
- [29] G. B. Osterhoudt, L. K. Diebel, M. J. Gray, X. Yang, J. Stanco, X. Huang, B. Shen, N. Ni, P. J. W. Moll, Y. Ran *et al.*, *Nat. Mater.* **18**, 471 (2019).
- [30] J. Ma, Q. Gu, Y. Liu, J. Lai, P. Yu, X. Zhuo, Z. Liu, J.-H. Chen, J. Feng, and D. Sun, *Nat. Mater.* **18**, 476 (2019).
- [31] L. Wu, S. Patankar, T. Morimoto, N. L. Nair, E. Thewalt, A. Little, J. G. Analytis, J. E. Moore, and J. Orenstein, *Nat. Phys.* **13**, 350 (2017).
- [32] Q. Wang, J. Zheng, Y. He, J. Cao, X. Liu, M. Wang, J. Ma, J. Lai, H. Lu, S. Jia *et al.*, *Nat. Commun.* **10**, 5736 (2019).
- [33] K. Takasan, T. Morimoto, J. Orenstein, and J. E. Moore, *Phys. Rev. B* **104**, L161202 (2021).

- [34] Y. Gao, S. Kaushik, E. J. Philip, Z. Li, Y. Qin, Y. P. Liu, W. L. Zhang, Y. L. Su, X. Chen, H. Weng *et al.*, *Nat. Commun.* **11**, 720 (2020).
- [35] B. Tilmann, A. K. Pandeya, G. Grinblat, L. D. S. Menezes, Y. Li, C. Shekhar, C. Felser, S. P. S. Parkin, A. Bedoya-Pinto, and S. A. Maier, *Adv. Mater.* **34**, 2106733 (2022).
- [36] H. K. Avetissian, *Relativistic Nonlinear Electrodynamics: The QED Vacuum and Matter in Super-Strong Radiation Fields* (Springer, Berlin, 2015).
- [37] N. Yoshikawa, T. Tamaya, and K. Tanaka, *Science* **356**, 736 (2017).
- [38] J. Lim, Y. S. Ang, F. J. García de Abajo, I. Kaminer, L. K. Ang, and L. J. Wong, *Phys. Rev. Research* **2**, 043252 (2020).
- [39] S. Kovalev, R. M. A. Dantas, S. Germanskiy, J.-C. Deinert, B. Green, I. Ilyakov, N. Awari, M. Chen, M. Bawatna, J. Ling *et al.*, *Nat. Commun.* **11**, 2451 (2020).
- [40] Y. Bai, F. Fei, S. Wang, N. Li, X. Li, F. Song, R. Li, Z. Xu, and P. Liu, *Nat. Phys.* **17**, 311 (2021).
- [41] Y.-Y. Lv, J. Xu, S. Han, C. Zhang, Y. Han, J. Zhou, S.-H. Yao, X.-P. Liu, M.-H. Lu, H. Weng *et al.*, *Nat. Commun.* **12**, 6437 (2021).
- [42] C. Shekhar, A. K. Nayak, Y. Sun, M. Schmidt, M. Nicklas, I. Leermakers, U. Zeitler, Y. Skourski, J. Wosnitza, Z. Liu *et al.*, *Nat. Phys.* **11**, 645 (2015).
- [43] N. Kumar, Y. Sun, N. Xu, K. Manna, M. Yao, V. Süß, I. Leermakers, O. Young, T. Förster, M. Schmidt *et al.*, *Nat. Commun.* **8**, 1642 (2017).
- [44] S. A. Mikhailov and K. Ziegler, *J. Phys.: Condens. Matter* **20**, 384204 (2008).
- [45] H. K. Avetissian, A. K. Avetissian, G. F. Mkrtchian, and K. V. Sedrakian, *Phys. Rev. B* **85**, 115443 (2012).
- [46] P. Bowlan, E. Martinez-Moreno, K. Reimann, T. Elsaesser, and M. Woerner, *Phys. Rev. B* **89**, 041408(R) (2014).
- [47] I. Al-Naib, J. E. Sipe, and M. M. Dignam, *Phys. Rev. B* **90**, 245423 (2014); *New J. Phys.* **17**, 113018 (2015).
- [48] L. A. Chizhova, F. Libisch, and J. Burgdorfer, *Phys. Rev. B* **94**, 075412 (2016); **95**, 085436 (2017).
- [49] H. K. Avetissian and G. F. Mkrtchian, *Phys. Rev. B* **97**, 115454 (2018).
- [50] Ó. Zurrón, A. Picón, and L. Plaja, *New J. Phys.* **20**, 053033 (2018).
- [51] C. Liu, Y. Zheng, Z. Zeng, and R. Li, *Phys. Rev. A* **97**, 063412 (2018).
- [52] Ó. Zurrón-Cifuentes, R. Boyero-García, C. Hernández-García, A. Picón, and L. Plaja, *Opt. Express* **27**, 7776 (2019).
- [53] S. A. Sato, H. Hirori, Y. Sanari, Y. Kanemitsu, and A. Rubio, *Phys. Rev. B* **103**, L041408 (2021).
- [54] X. Q. Wang and X. B. Bian, *Phys. Rev. A* **103**, 053106 (2021).
- [55] Y. Zhang, L. Li, J. Li, T. Huang, P. Lan, and P. Lu, *Phys. Rev. A* **104**, 033110 (2021).
- [56] F. Dong, Q. Xia, and J. Liu, *Phys. Rev. A* **104**, 033119 (2021).
- [57] Y. Feng, S. Shi, J. Li, Y. Ren, X. Zhang, J. Chen, and H. Du, *Phys. Rev. A* **104**, 043525 (2021).
- [58] M. S. Mrudul and G. Dixit, *Phys. Rev. B* **103**, 094308 (2021).
- [59] H. K. Avetissian, G. F. Mkrtchian, and A. Knorr, *Phys. Rev. B* **105**, 195405 (2022).
- [60] A. Bharti, M. S. Mrudul, and G. Dixit, *Phys. Rev. B* **105**, 155140 (2022).
- [61] R. M. A. Dantas, Z. Wang, P. Surowka, and T. Oka, *Phys. Rev. B* **103**, L201105 (2021).
- [62] C. Zeng, S. Nandy, and S. Tewari, *Phys. Rev. B* **103**, 245119 (2021).
- [63] F. Nematollahi, S. A. Oliaei Motlagh, V. Apalkov, and M. I. Stockman, *Phys. Rev. B* **99**, 245409 (2019).
- [64] M. Nakahara, *Geometry, Topology, and Physics*, 2nd ed. (CRC, Boca Raton, 2003).
- [65] H. B. Nielsen and M. Ninomiya, *Nucl. Phys. B* **185**, 20 (1981).
- [66] L. Yue and M. B. Gaarde, *Phys. Rev. A* **101**, 053411 (2020).